

# Dynamics and stability in optical communication networks: a system theory framework<sup>☆</sup>

Lacra Pavel<sup>a,\*</sup>

<sup>a</sup>*Department of Electrical and Computer Engineering, University of Toronto, Toronto, ONT, Canada M5S 3G4*

Received 19 March 2003; received in revised form 27 December 2003; accepted 29 March 2004

## Abstract

This paper addresses the problem of dynamics analysis in optical networks from a system control perspective. A general framework for finding the transfer matrix representation of an optical network is developed, based on linear fractional transformations. Under the natural assumption of equal time-delay for all channels in a link, the network transfer matrix is simplified such that channel cross-coupling is evidenced. The optical network stability problem is then reformulated as a robust stability problem and stability conditions are developed by applying  $\mu$ -analysis.

© 2004 Elsevier Ltd. All rights reserved.

*Keywords:* Communication networks; Optical communication systems; Interconnected dynamics; Time-delay systems; Stability analysis

## 1. Introduction

In the context of evolution from optical point-to-point communication links towards reconfigurable optical networks, dynamic aspects in optical networks have started to be considered very recently, as in [Bala and Brackett \(1996\)](#), [Mukherjee \(2000\)](#) and [Barnes \(2002\)](#). Reconfigurable optical networks operate in a dynamic environment, with existing channels being continuously in-service while network reconfiguration (channel add/drop) is being performed. Such optical networks are in fact large-scale, time-delay dynamical systems, with channel add/drop acting as a disturbance for the existent channels. This paper addresses the problem of dynamic response analysis in optical networks from a system and control theory perspective.

In optical communications, information is transmitted by modulating the optical power of light pulses of a specific frequency (wavelength). Multichannel optical systems are realized by wavelength division multiplexing (WDM), which consists of several sources multiplexed in the wavelength

domain. Optical signals, corresponding to multiple channels at different wavelengths, are transmitted together on a single optical fiber. Each channel's information is recovered at the receiver after demultiplexing and conversion from optical to electrical domain. An essential parameter in determining the performance of an optical communication system is the optical power per channel. Optical signals experience power loss during propagation through an optical fiber, which is compensated by using optical amplifiers every few tens of km.

The need to study dynamics and dynamic effects in optical networks is motivated by two important facts. Firstly, the presence of optical amplifiers which have active control, together with their operation in reconfiguration scenarios introduces a time-dependent component. The most widely used multichannel optical amplifier is the Erbium-doped fiber amplifier (EDFA), firstly studied from a dynamical point of view in [Sun, Zyskind, and Srivastava \(1997\)](#). Due to their slow gain-dynamics, EDFAs do not introduce any channel cross-talk (cross-coupling), at the high bit-rates used in optical communications. EDFAs react only to variation in average optical signal power. However in dynamically reconfigurable networks, channel add/drop and hence changes in optical signal power, occur on time-scales comparable with the EDFA time-constant. This requires consideration of dynamics as well as transient control in optical amplifiers, see for example [Sun et al. \(1997\)](#), [Srivastava, Sun, Zyskind, and](#)

<sup>☆</sup> This paper was not presented at any IFAC meeting. This paper was recommended for publication in revised form by Associate Editor Hitay Ozbay under the direction of Editor Tamer Başar. This work was supported by the Natural Sciences and Engineering Research Council of Canada.

\* Corresponding author. Tel.: +1-416-946-8662; fax: +1-416-978-0804.

E-mail address: [pavel@control.toronto.edu](mailto:pavel@control.toronto.edu) (L. Pavel).

Sulhoff (1997) and Pavel (2003). Other devices such as dynamic equalizing filters (see Ford & Walker, 1998), are also used to adjust optical power profile in wavelength domain. This enables all channels to reach the receiver with equal optical power, and hence with equal optical signal-to-noise ratio. Effectively, an optical link is a multivariable dynamical system composed from cascaded dynamical optical elements.

Secondly, for reconfigurable optical networks, mesh type configurations can be realized, not only link configurations. Since channel routes can be changed dynamically via channel add/drop or switching, closed cycles can be formed, (see Bala & Brackett, 1996), and time-delay effects need to be considered. Network reconfiguration, failures or protection switching can cause abrupt changes in optical power across some wavelengths, which can be transferred to other wavelengths. Due to dynamic cross-coupling effects as well as due to propagation time-delay, for ring-type configurations, bursts of power fluctuations occur, resulting in possible network instability. This was shown recently in simulation and experimental studies, as in Yoo, Xin, and Garrett (1998), Kim, Bae, Joon Ahn, and Park (2000), Pavel (2002). The resulting dynamic behavior of such a network is complex and, to the best of our knowledge, no analytical network dynamics studies exist.

In conventional switched communication networks, dynamics is an important aspect of the data-layer, in terms of traffic congestion, control and stability, (see Altman, Basar, & Srikant, 1999; Alpcan & Basar, 2002; Wang & Paganini, 2002). In these networks, channels are characterized by static loss/gain only. Given the inherent dynamics of an optical link, optical network dynamics is an important aspect even at the physical layer. The analytical study of optical network dynamics is the problem considered in this paper. For tractability, linearized models are assumed.

The paper is organized as follows. In Section 2, we formulate the problem for a generic optical network in ring-type configuration. In Section 3, we find the network transfer matrix, in terms of a modified Redheffer star-product with propagation delay feedback. We specialize these results for transient response analysis under channel add/drop. In Section 4, we address the network stability by reformulating it as a robust stability problem and resorting to  $\mu$ -analysis. Simulation results are shown in Section 5, with conclusions being given in Section 6.

**2. Problem formulation**

The following general notations are defined. Assume as in general network theory, (see Anderson, 1973), that the optical network is characterized by a set of nodes, a set of optical links  $\mathcal{L} = \{1, \dots, L\}$  connecting the nodes, and a set of channels,  $\mathcal{M} = \{1, \dots, m\}$ . Optical add-drop multiplexers (OADM) that are used to separate and recombine wavelength channels, constitute network nodes. The input to each

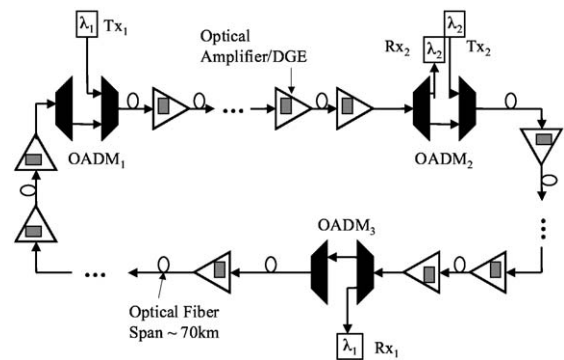


Fig. 1. Optical network—quasi-ring configuration.

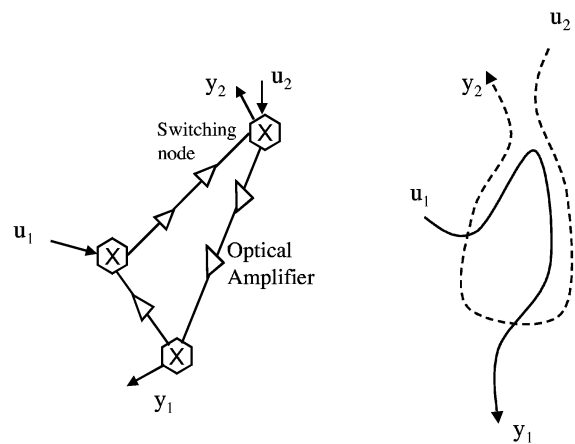


Fig. 2. Quasi-ring configuration: schematic and optical paths.

optical link is either from optical sources (Tx) or from other optical links, via the OADM (switching) nodes. In what follows, we consider a generic optical network configuration as in Fig. 1, corresponding to three OADM nodes. The topology is schematically shown in Fig. 2, with the corresponding optical paths. Such a ring-type topology, with partially closed loops being formed between channel optical paths, is called a quasi-ring topology. It is representative for selected paths extracted from a mesh configuration, and it is similar to those considered in network reconfiguration studies, (see Bala & Brackett, 1996; Yoo et al., 1998; Pavel, 2002). Special cases of completely closed ring configurations (see Kim et al., 2000), can be realized by modifications of this diagram. We assume the  $m$  channels are separated in two wavelength sets,  $\lambda_1$  and  $\lambda_2$ , each with  $m_1$  and  $m_2$  channels,

$$\lambda_1 = \{\lambda_{1,1}, \dots, \lambda_{1,m_1}\}, \quad \lambda_2 = \{\lambda_{2,1}, \dots, \lambda_{2,m_2}\}. \quad (1)$$

This partitioning in two sets is the simplest case that can evidence coupling between channels. Without loss of generality we assume that  $\lambda_1$  and  $\lambda_2$  sets are ordered. From Fig. 1, channels  $\lambda_1$  are added (transmitted) at the Tx<sub>1</sub> site (OADM<sub>1</sub>) and dropped (received) at the Rx<sub>1</sub> site (OADM<sub>3</sub>). Channels  $\lambda_2$  are added at the Tx<sub>2</sub> site (OADM<sub>2</sub>) and dropped at the Rx<sub>2</sub> site (OADM<sub>2</sub>).

We denote by  $N_l$  the number of optical spans in link  $l \in \mathcal{L}$ , with  $N_l \in \mathcal{N}$ ,  $\mathcal{N} = \{1, \dots, N\}$ . Each optical link between two adjacent OADM nodes has several optically amplified spans. An optically amplified span consists of optical fiber and in-line optical amplifiers or dynamic optical amplifiers. An in-line optical amplifier is controlled to maintain either a constant launched average output power or a constant gain. Around an operating point defined by the nominal average channel power, the linearized model is denoted by  $G_{\text{OA}}$ .  $G_{\text{OA}}$  is a MIMO, square LTI transfer matrix, (see Sun et al., 1997; Pavel, 2003), with high-pass diagonal terms and low-pass off-diagonal terms, and with typical time-constants of 1–10 ms. Thus, on time-scales relevant to network reconfiguration, channel cross-coupling can exist. Dynamic optical amplifiers are realized by combining optical amplifiers with dynamic gain equalizer filters (DGE). These filters with spectrally adjustable attenuation are used for dynamically equalizing channel powers, as in Ford and Walker (1998) and Pavel (2003).

In what follows, we assume that an optical span is described by an overall transfer matrix, combining the transfer matrices of optical amplifiers, filters, and fiber.

Let  $u$  and  $y$  denote the vectors of average optical power at the network input and output, respectively, partitioned accordingly to the two wavelength sets,  $\lambda_1, \lambda_2$ ,

$$u = \begin{bmatrix} u_1 \\ u_2 \end{bmatrix}, \quad y = \begin{bmatrix} y_1 \\ y_2 \end{bmatrix}, \quad u_{1,2}, y_{1,2} \in R^{m_{1,2}}. \quad (2)$$

Based on this setup, we formulate the problem of finding the transfer matrix between  $u$  and  $y$ , (2), for the optical network (Figs. 1 or 2). Furthermore, we seek to study cross-coupling effects between the two groups of wavelengths, and also to analyze the network stability.

As notation, let a square LTI system  $G$  be given as

$$G : \begin{cases} \dot{x} = Ax + Bu_g, \\ y_g = Cx + Du_g, \end{cases} \quad G(s) = \begin{bmatrix} A|B \\ C|D \end{bmatrix}, \quad (3)$$

where  $x \in R^n$  is the state vector,  $u_g, y_g \in R^m$  are the input and output vectors, respectively. We use the standard equivalence between state-space and transfer matrix  $G(s)$ , with the variable  $s$  being often omitted for simplicity. As in (2), let  $u_g, y_g$ , (3), be partitioned as

$$u_g = \begin{bmatrix} u_{g1} \\ u_{g2} \end{bmatrix}, \quad y_g = \begin{bmatrix} y_{g1} \\ y_{g2} \end{bmatrix}, \quad u_g, y_g \in R^{(m_1+m_2)}. \quad (4)$$

From the system  $G$ ,  $y_g = Gu_g$ , we define a related system,  $\tilde{G}$ , that maps the same input vector,  $u_g$ , to the reversed output vector,  $\tilde{y}_g$ , such that

$$\tilde{y}_g = \tilde{G} u_g, \quad \tilde{y}_g = \begin{bmatrix} y_{g2} \\ y_{g1} \end{bmatrix}, \quad \tilde{y}_g \in R^{(m_2+m_1)}. \quad (5)$$

Notice that in state-space representation, systems  $G$  and  $\tilde{G}$  have the same state equations, and only the output equations are reversed, i.e., as input–output relationship

$$\tilde{G} = \begin{bmatrix} 0 & I_{m_2} \\ I_{m_1} & 0 \end{bmatrix} G. \quad (6)$$

### 3. Optical network transfer matrix

In this section we find a closed form of the optical network transfer matrix. We start by finding optical span and optical link transfer matrices. We show how the distributed multichannel time-delay can be lumped on a link-by-link basis. The network transfer matrix is then determined by applying linear fractional techniques. Next we show that network dynamics depends explicitly on time-delay along the optical path and on channel group cross-coupling across the network.

Consider the general configuration in Fig. 1, with notations as in the previous section. Recall that each optical link between two adjacent optical add-drop sites (nodes), is composed of cascading several optically amplified spans. Across an optical span, between any two optical amplifier sites, optical signals experience power loss and delay due to propagation through the optical fiber. Let  $u_s(t)$  and  $y_s(t)$  denote the optical power vector at the input and at the output of an optical span, respectively. Then the following relation holds

$$\begin{bmatrix} y_{s,1}(t) \\ \vdots \\ y_{s,m}(t) \end{bmatrix} = \begin{bmatrix} \alpha_1 & \cdots & 0 \\ & \ddots & \\ 0 & \cdots & \alpha_m \end{bmatrix} \begin{bmatrix} u_{s,1}(t - \tau_1) \\ \vdots \\ u_{s,m}(t - \tau_m) \end{bmatrix}, \quad (7)$$

where  $\alpha_i$  and  $\tau_i$ ,  $i = 1, \dots, m$ , are channel fiber loss coefficients and propagation time-delays, respectively.

Channel fiber loss coefficients are typically the same and are denoted here by  $\alpha$ . With respect to the propagation time-delay we use the following assumption.

(A1): All channels in an optical span (link) experience essentially the same propagation time-delay.

This is justified as follows. In an optical span (link), different channels (wavelengths) share the optical fiber and travel across the same distance. Since optical spans have typical lengths of tens of kilometers, propagation-induced delay is on the order of fractions of ms. Due to chromatic dispersion, (see Agrawal, 2002), different wavelengths travel with slightly different speeds and experience slightly different delays. However, for adequate receiver detection, dispersion management techniques are used periodically in any optical system, see Agrawal (2002). As a result, dispersion induced delay (pulse broadening) is maintained at a fraction of the bit period (typically fractions of ns). Thus, on network reconfiguration time-scales, from  $\mu\text{s}$  to hundreds of ms, dispersion-induced delay differences are negligible compared to the average propagation delay, and (A1) is valid.

From (7) and (A1) it follows that

$$y_s(s) = \alpha \mathcal{D}_\tau(s) u_s(s), \quad \mathcal{D}_\tau(s) = e^{-\tau s} I_m, \quad (8)$$

where  $\alpha$  and  $\tau$  are the fiber loss coefficient and the propagation delay, respectively.

Recall that an optical amplifier is described by a MIMO LTI transfer matrix, denoted  $G_{OA}$ , (see Sun et al., 1997; Pavel, 2003). Let  $G_{(k)}(s)$ , denote the transfer matrix of the  $k$ th optically amplified span, that combines the optical amplifier transfer matrix ( $G_{OA}$ ), and the fiber loss coefficient ( $\alpha$ ). Then the overall span transfer matrix, including the delay effects, is given as

$$G_{\mathcal{D},(k)}(s) = G_{(k)}(s) \mathcal{D}_\tau(s), \quad (9)$$

where  $\mathcal{D}_\tau(s)$  is defined in (8). For an optical link with  $N$  optically amplified spans, the link transfer is given next.

**Lemma 1.** Consider an optical link realized by a series interconnection of  $N$  optical spans, each span having a transfer matrix,  $G_{\mathcal{D},(k)}(s)$ , (9), corresponding to a time-delay  $\tau$  per span, by (A1). Then the optical link has a transfer matrix  $S_{\mathcal{D}}(s)$  given as

$$S_{\mathcal{D}}(s) = \mathcal{D}_N(s) S(s),$$

$$\text{where } S(s) = \prod_{k=1}^N G_{(k)}(s), \quad \mathcal{D}_N(s) = e^{-(N\tau)s} I_m.$$

**Proof.** We use the fact that in any LTI system,  $G(s)$ , when all channels have the same time-delay, then delay at the input is equivalent to delay at the output, i.e.,

$$G(s) \mathcal{D}_\tau(s) = \mathcal{D}_\tau(s) G(s). \quad (10)$$

For an optical link with  $N$  spans we have

$$S_{\mathcal{D}}(s) = \prod_{k=1}^N G_{\mathcal{D},(k)}(s), \quad (11)$$

which, using (9) and (10), can be rewritten as

$$S_{\mathcal{D}}(s) = \prod_{k=1}^N G_{(k)}(s) \prod_{k=1}^N \mathcal{D}_\tau(s). \quad (12)$$

The result follows immediately using  $\prod_{k=1}^N \mathcal{D}_\tau(s) = e^{-(N\tau)s} I_m$  and the given notations.  $\square$

Lemma 1 shows that under (A1), the distributed time-delays can be lumped together on a link-by-link basis.

With this result, let  $P_{\mathcal{D}}$ ,  $Q_{\mathcal{D}}$  and  $X_{\mathcal{D}}$  be the optical link transfer matrices in Fig. 1, be given as in Lemma 1. Recall that  $u$  and  $y$ , (2), denote the network input and output optical power vectors, partitioned accordingly to  $\lambda_1$  and  $\lambda_2$ . Then the equivalent network block diagram for Fig. 1 is shown in Fig. 3.

The following result gives a closed-form for the optical network transfer matrix (Fig. 4).

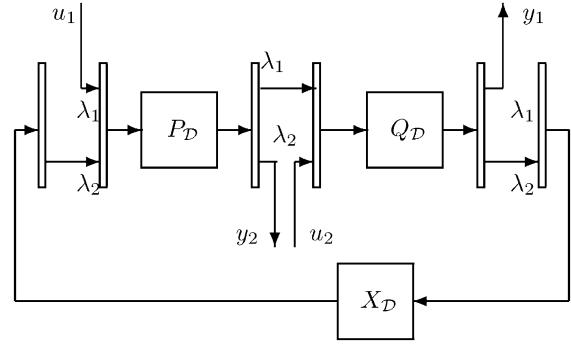


Fig. 3. Optical network block-diagram.

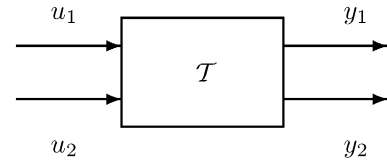


Fig. 4. Two-port network representation.

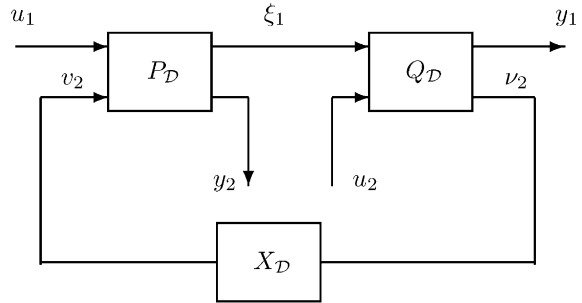


Fig. 5.

**Theorem 2.** Under (A1) the optical network transfer matrix,  $\mathcal{F}$ , of Fig. 1 (Fig. 3),

$$\begin{bmatrix} y_1 \\ y_2 \end{bmatrix} = \mathcal{F} \begin{bmatrix} u_1 \\ u_2 \end{bmatrix}$$

is

$$\mathcal{F} = \begin{bmatrix} 0 & I_{m_1} \\ I_{m_2} & 0 \end{bmatrix} \mathfrak{R} \left( \begin{bmatrix} 0 & I_{m_2} \\ I_{m_1} & 0 \end{bmatrix} P_{\mathcal{D}}, \begin{bmatrix} 0 & X_{\mathcal{D}} \\ I_{m_1} & 0 \end{bmatrix} Q_{\mathcal{D}} \right),$$

where  $P_{\mathcal{D}}$ ,  $Q_{\mathcal{D}}$ , and  $X_{\mathcal{D}}$  denote the optical link transfer matrices as in Lemma 1, and  $\mathfrak{R}(\cdot, \cdot)$  is the Redheffer star-product (see Zhou, Doyle, & Glover, 1996).

**Proof.** We prove this result by rearranging the network block diagram in Fig. 3 in a convenient way and then applying linear fractional techniques. By combining each half of an add-drop site with the adjacent optical link, Fig. 3 can be redrawn as in Fig. 5.

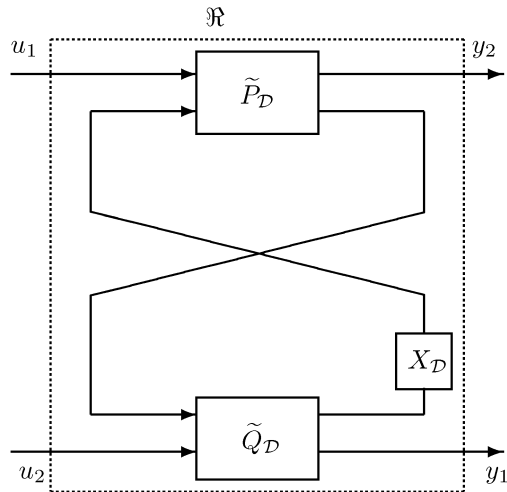


Fig. 6. Network representation: star-product configuration.

Fig. 5 is equivalent to the interconnected system in Fig. 6. This is seen by switching the output order of  $P_{\mathcal{D}}$  and using (5) for the reversed output system,  $\tilde{P}_{\mathcal{D}}$ .

The closed-loop system in Fig. 6 is described by

$$\begin{bmatrix} y_2 \\ y_1 \end{bmatrix} = \mathfrak{R}(\tilde{P}_{\mathcal{D}}, \tilde{R}_{\mathcal{D}}) \begin{bmatrix} u_1 \\ u_2 \end{bmatrix}$$

with  $\mathfrak{R}(\cdot)$  the Redheffer star-product and  $\tilde{R}_{\mathcal{D}}$  defined as

$$\tilde{R}_{\mathcal{D}} = \begin{bmatrix} X_{\mathcal{D}} & 0 \\ 0 & I_{m_1} \end{bmatrix} \tilde{Q}_{\mathcal{D}}. \quad (13)$$

Therefore

$$\begin{bmatrix} y_1 \\ y_2 \end{bmatrix} = \begin{bmatrix} 0 & I_{m_1} \\ I_{m_2} & 0 \end{bmatrix} \mathfrak{R}(\tilde{P}_{\mathcal{D}}, \tilde{R}_{\mathcal{D}}) \begin{bmatrix} u_1 \\ u_2 \end{bmatrix} \quad (14)$$

and the result follows by using (13), and the definition of the reversed output systems  $\tilde{P}_{\mathcal{D}}$  and  $\tilde{Q}_{\mathcal{D}}$  as in (6).  $\square$

**Remark 1.** Theorem 2 gives a closed form for the transfer matrix of the optical network as a two-port system. This expression is particularly useful as it is based on linear fractional transformations (LFT) with their interconnection properties, (see Zhou et al., 1996). This result could be used to find directly the optical network state-space representation. Alternatively, a scattering-matrix representation can be found as in the case of electrical networks (see Anderson, 1973).

**Remark 2.** Theorem 2 is developed for a generic network as in Fig. 1 (or Fig. 2), where add and drop is done via three OADM nodes. It can be shown that any possible quasi-closed cycle configuration that involves coupling between two groups of wavelengths can be reduced to this configuration, and hence to Theorem 2.

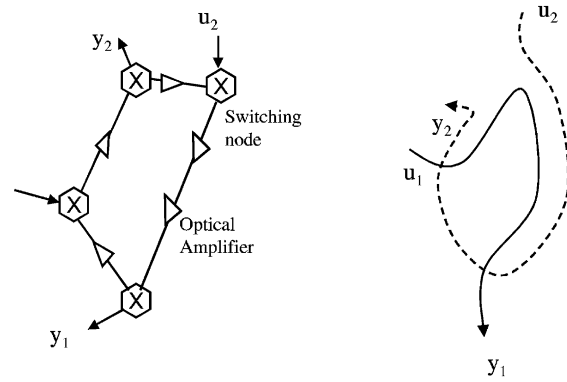


Fig. 7. Quasi-ring configuration (four nodes).

For example, one possible configuration has two nodes, and add-drop is done at the same site (as for OADM2). This is a special case of Fig. 1 (Fig. 3), that can be obtained by setting  $X_{\mathcal{D}} = I_{m_2}$  in Fig. 3 and Theorem 2.

Another possible configuration has four nodes (see Fig. 7), where each group is added and dropped at a different node. This can be reduced to Fig. 3, by using Fig. 7 and Fig. 2. In this case, group  $\lambda_1$  propagates through an extra link,  $X_{\mathcal{D},1}$ , similar to the  $\lambda_2$  group propagating via the  $X_{\mathcal{D}}$  link in Fig. 3. The network transfer matrix is given as in Theorem 2 with  $P_{\mathcal{D}}$  replaced by

$$\hat{P}_{\mathcal{D}} = \begin{bmatrix} X_{\mathcal{D},1} & 0 \\ 0 & I_{m_2} \end{bmatrix} P_{\mathcal{D}}.$$

More complex configurations could be studied by decomposition into basic configurations as in Fig. 2 (or Fig. 1), followed by interconnection of the two-port forms (Fig. 4), and use of LFT properties. Such an example diagram is shown in Fig. 8(a) and (b).

**Remark 3.** An alternative transfer matrix representation of the network can be obtained by using the connection matrix concept as in switched communications networks (see Alpcan & Basar, 2002; Wang & Paganini, 2002). We indicate next how to obtain such an overall description. The input to each of the  $L$  links is either from sources or from other links. Define an  $(L \times m)$  source-to-link connection matrix  $F$ , that maps source channels to links, with

$$F_{j,i} = \begin{cases} 1 & \text{if channel } i \\ & \text{uses link } j, & i \in \mathcal{M}, j \in \mathcal{L} \\ 0 & \text{otherwise} \end{cases} \quad (15)$$

and a diagonal  $(m \times m)$  link-to-link interconnection matrix,  $H_{l,j}$ , with the diagonal element for channel  $i$

$$h_{l,j}(i) = \begin{cases} 1 & \text{if link } j \text{ is connected} \\ & \text{to link } l, & i \in \mathcal{M}, l, j \in \mathcal{L}. \\ 0 & \text{otherwise.} \end{cases} \quad (16)$$

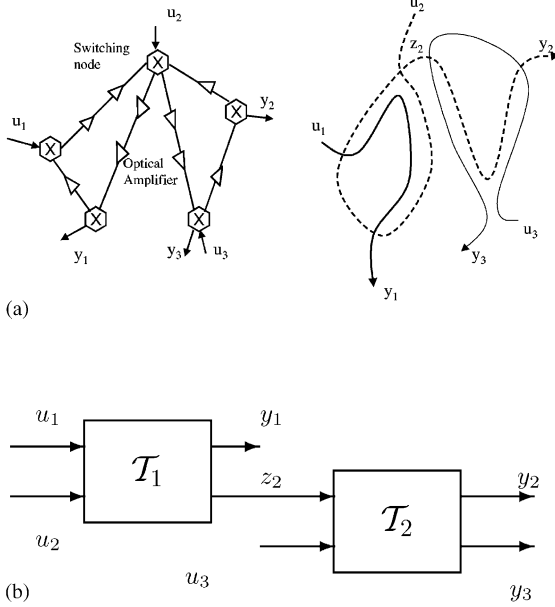


Fig. 8. More complex configuration: (a) decomposition, (b) two-port interconnection.

Then it can be shown that for all the links we can write

$$u_L = H_x y_L + F_x u, \tag{17}$$

with

$$u_L = \begin{bmatrix} u_{L_1} \\ \vdots \\ u_{L_L} \end{bmatrix}, \quad u_{L_j} = \begin{bmatrix} u_{L_{j,1}} \\ \vdots \\ u_{L_{j,m}} \end{bmatrix}$$

and similar for  $y_L, y_{L_j}$ . In (17),  $u_L, y_L$  are the augmented,  $mL$ -dimensional, link input and output vectors, while  $H_x, F_x$  are the full block matrices for link-to-link and source-to-link interconnection.  $H_x$  and  $F_x$  can be defined appropriately from  $H_{l,j}$ , (16), and  $F_{j,i}$ , (15), respectively. From Lemma 1, for link  $l$  we have  $y_{L_l} = S_{\mathcal{Q},l}(s)u_{L_l}$ , so that  $y_L(s) = S_{\mathcal{Q},x}(s)u_L(s)$  with

$$S_{\mathcal{Q},x}(s) = \begin{bmatrix} S_{\mathcal{Q},1}(s) & \cdots & 0 \\ & \ddots & \\ 0 & \cdots & S_{\mathcal{Q},L}(s) \end{bmatrix}. \tag{18}$$

Similarly to  $H_x, F_x$ , we can define a link-to-output connection matrix,  $J_x$ , so that

$$y = J_x y_L. \tag{19}$$

Using (17)–(19), the network transfer matrix between  $u$  and  $y$  can be written as

$$\mathcal{F}(s) = J_x (I_{mL} - S_{\mathcal{Q},x}(s)H_x)^{-1} S_{\mathcal{Q},x} F_x u. \tag{20}$$

This is a general representation, that has however a large inner dimensionality, i.e.,  $(mL \times mL)$  as opposed to  $(m \times m)$ . In addition it does not provide a direct way of analyzing stability, nor any direct insight into network dynamics as given by Theorem 2.

In what follows, we use Theorem 2 to show that network dynamics depends explicitly on the coupling between the two groups, and on the total network time-delay. Recall Fig. 3 and partition  $P_{\mathcal{Q}}$  and  $Q_{\mathcal{Q}}$  accordingly to  $\lambda_1, \lambda_2$

$$P_{\mathcal{Q}} = \begin{bmatrix} P_{\mathcal{Q},11} & P_{\mathcal{Q},12} \\ P_{\mathcal{Q},21} & P_{\mathcal{Q},22} \end{bmatrix}, \quad Q_{\mathcal{Q}} = \begin{bmatrix} Q_{\mathcal{Q},11} & Q_{\mathcal{Q},12} \\ Q_{\mathcal{Q},21} & Q_{\mathcal{Q},22} \end{bmatrix}. \tag{21}$$

Assuming that the optical links  $P_{\mathcal{Q}}, Q_{\mathcal{Q}}$  and  $X_{\mathcal{Q}}$  are composed of  $N_1, N_2$  and  $N_3$  optical fiber spans, respectively, then from Lemma 1 we have

$$\begin{aligned} P_{\mathcal{Q}}(s) &= \mathcal{D}_{N_1}(s)P(s), & Q_{\mathcal{Q}}(s) &= \mathcal{D}_{N_2}(s)Q(s), \\ X_{\mathcal{Q}}(s) &= \mathcal{D}_{N_3}(s)X(s), \end{aligned} \tag{22}$$

where  $P, Q, X$  are link transfer matrices without delay

$$\begin{aligned} P(s) &= \prod_{k=1}^{N_1} G_{(k)}(s), & Q(s) &= \prod_{k=1}^{N_2} G_{(k)}(s), \\ X(s) &= \prod_{k=1}^{N_3} G_{(k),22}(s), \end{aligned}$$

and  $\mathcal{D}_{N_i}(s) = e^{-(N_i \tau)s} I_m$ . Then, an equivalent network transfer matrix is given next.

**Theorem 3.** Under (A1), for the system  $P_{\mathcal{Q}}, Q_{\mathcal{Q}}$  as in (21), the overall network transfer matrix  $\mathcal{F}$  between  $u$  and  $y$  can be represented as

$$\begin{bmatrix} y_1 \\ y_2 \end{bmatrix} = \mathcal{F} \begin{bmatrix} u_1 \\ u_2 \end{bmatrix}, \quad \mathcal{F} = \begin{bmatrix} \mathcal{F}_{11} & \mathcal{F}_{12} \\ \mathcal{F}_{21} & \mathcal{F}_{22} \end{bmatrix}$$

with  $\mathcal{F}_{ij}, i, j = 1, 2$  being defined as

$$\begin{aligned} \mathcal{F}_{11} &= Q_{\mathcal{Q},11} \Psi_{\mathcal{Q}} P_{\mathcal{Q},11}, \\ \mathcal{F}_{12} &= Q_{\mathcal{Q},12} + Q_{\mathcal{Q},11} P_{\mathcal{Q},12} \tilde{\Psi}_{\mathcal{Q}} X_{\mathcal{Q}} Q_{\mathcal{Q},22}, \\ \mathcal{F}_{21} &= P_{\mathcal{Q},21} + P_{\mathcal{Q},22} X_{\mathcal{Q}} Q_{\mathcal{Q},21} \Psi_{\mathcal{Q}} P_{\mathcal{Q},11}, \\ \mathcal{F}_{22} &= P_{\mathcal{Q},22} \tilde{\Psi}_{\mathcal{Q}} X_{\mathcal{Q}} Q_{\mathcal{Q},22} \end{aligned} \tag{23}$$

and  $\Psi_{\mathcal{Q}}, \tilde{\Psi}_{\mathcal{Q}}$  being sensitivity-like transfer matrices

$$\begin{aligned} \Psi_{\mathcal{Q}} &= (I - P_{\mathcal{Q},12} X_{\mathcal{Q}} Q_{\mathcal{Q},21})^{-1}, \\ \tilde{\Psi}_{\mathcal{Q}} &= (I - X_{\mathcal{Q}} Q_{\mathcal{Q},21} P_{\mathcal{Q},12})^{-1}. \end{aligned}$$

**Proof.** Recall from Zhou et al. (1996), that for two correspondingly partitioned systems  $G$  and  $H$

$$G = \begin{bmatrix} G_{11} & G_{12} \\ G_{21} & G_{22} \end{bmatrix}, \quad H = \begin{bmatrix} H_{11} & H_{12} \\ H_{21} & H_{22} \end{bmatrix}$$

the Redheffer star-product,  $\mathfrak{R}(G, H)$  is defined as

$$\mathfrak{R}(G, H) = \begin{bmatrix} F_l(G, H_{11}) & G_{12}(I - H_{11}G_{22})^{-1}H_{12} \\ H_{21}(I - G_{22}H_{11})^{-1}G_{21} & F_u(H, G_{22}) \end{bmatrix},$$

where  $F_l(G, H_{11})$  ( $F_u(H, G_{22})$ ) is the lower (upper) linear fractional transformation (LFT)

$$F_l(G, H_{11}) = G_{11} + G_{12}H_{11}(I - G_{22}H_{11})^{-1}G_{21},$$

$$F_u(H, G_{22}) = H_{22} + H_{21}G_{22}(I - H_{11}G_{22})^{-1}H_{12}.$$

Then using Theorem 2 and (21) it follows that

$$\mathfrak{R}(\tilde{P}_{\mathcal{D}}, \tilde{R}_{\mathcal{D}}) = \begin{bmatrix} F_l(\tilde{P}_{\mathcal{D}}, X_{\mathcal{D}}Q_{\mathcal{D},21}) & P_{\mathcal{D},22}\tilde{\Psi}_{\mathcal{D}}X_{\mathcal{D}}Q_{\mathcal{D},22} \\ Q_{\mathcal{D},11}\Psi_{\mathcal{D}}P_{\mathcal{D},11} & F_u(\tilde{R}_{\mathcal{D}}, P_{\mathcal{D},12}) \end{bmatrix},$$

where

$$F_l(\tilde{P}_{\mathcal{D}}, X_{\mathcal{D}}Q_{\mathcal{D},21}) = P_{\mathcal{D},21} + P_{\mathcal{D},22}X_{\mathcal{D}}Q_{\mathcal{D},21}\Psi_{\mathcal{D}}P_{\mathcal{D},11},$$

$$F_u(\tilde{R}_{\mathcal{D}}, P_{\mathcal{D},12}) = Q_{\mathcal{D},12} + Q_{\mathcal{D},11}P_{\mathcal{D},12}\tilde{\Psi}_{\mathcal{D}}X_{\mathcal{D}}Q_{\mathcal{D},22}$$

and  $\tilde{R}_{\mathcal{D}}$  and  $\Psi_{\mathcal{D}}, \tilde{\Psi}_{\mathcal{D}}$  as in (13), (23), were used. Then the result follows immediately.  $\square$

Note that typically link transfer matrices  $Q_{i,j}, P_{i,j}, i, j = 1, 2, i \neq j$  are strictly proper. This follows since the amplifier transfer matrix (see Sun et al., 1997; Pavel, 2003), does not have any high-frequency cross-talk. Therefore, since both  $\Psi_{\mathcal{D}}$  and  $\tilde{\Psi}_{\mathcal{D}}$  exist, the above network representation is well-defined as a star-product.

Based on star-product properties, an optical network state-space representation can be found, by using state-space descriptions of individual optical spans (links) and an LTI approximation for the pure time-delay part.

**Remark 4.** Theorem 3 provides insight into the network dynamics. Note that coupling between the two sets of wavelength is due to the cross-transfer matrices across optical links, e.g.,  $Q_{12}$  and  $P_{21}$ . When these cross-term factors are identically null for all frequencies, there is no wavelength coupling, equivalent to the network transfer matrix having a block diagonal form. This means that there will be no delay induced effects to be propagated from one group to another, corresponding to perfect decoupling between channels. This is the case of typical electrical switched networks, which do not have link dynamics, but only static gain coefficients.

**Remark 5.** Note that the distributed time-delay in (23) can be lumped along a path using Lemma 1 as in (22). For example for the  $\mathcal{T}_{12}$  matrix block we can write

$$\mathcal{T}_{12} = \mathcal{D}^{N_2}(Q_{12} + \mathcal{D}^{N_1}Q_{11}P_{12}\tilde{\Psi}_{\mathcal{D}}XQ_{22}),$$

where  $\mathcal{D}^{N_t} = e^{-N_t\tau}$ ,  $N_t = N_1 + N_2 + N_3$ , and  $\tau_t = N_t\tau$  is the total network propagation delay.

**Remark 6.** Theorem 3 can be used to study network transient response at dynamic reconfiguration (sudden channel add/drop). Cross-talk between two groups of wavelengths can be regarded as a disturbance rejection problem in frequency domain, with performance given by the  $H_{\infty}$  norm of the off-diagonal terms in (23). For the case of dynamic power changes on channels in  $\lambda_2$ , the effect on the channels in  $\lambda_1$  set, i.e., on  $y_1$ , can be determined by using the transfer matrix from  $u_2$  to  $y_1$ ,  $\mathcal{T}_{12}$ , and its  $H_{\infty}$  norm, since

$$\|y_1\|_2 = \|\mathcal{T}_{12}\|_{\infty}\|u_2\|_2.$$

#### 4. Stability analysis framework

In addition to being useful for analyzing optical network dynamic response, Theorem 3 can be used to address the optical network stability analysis. This problem will be considered in this section, by reformulating it as a robust stability problem and solving it via  $\mu$ -analysis.

An underlying basic assumption is that all optical links are stable systems, so that from (23) in Theorem 3 it follows that the internal stability of the overall optical network is equivalent to stability of  $\Psi_{\mathcal{D}}$ , (23),

$$\Psi_{\mathcal{D}} = (I - P_{\mathcal{D},12}X_{\mathcal{D}}Q_{\mathcal{D},21})^{-1}. \quad (24)$$

Conditions for stability of  $\Psi_{\mathcal{D}}$ , (24), can be found by representing it in a feedback configuration as in Fig. 9(a), and by applying the standard small gain theorem.

Specifically,  $\Psi_{\mathcal{D}}$  is internally stable if and only if the  $H_{\infty}$  norm of the loop-transfer matrix is less than unity. Applying Lemma 1 to individual terms in (24), we separate

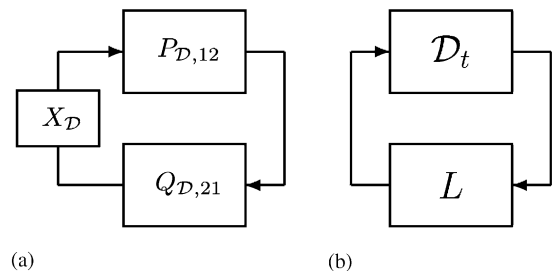


Fig. 9. Loop configuration for network stability.

the time-delay blocks as in (22), and lump them as

$$\mathcal{D}_t = e^{-\tau_t s} I_{m_1}, \quad \tau_t = (N_1 + N_2 + N_3) * \tau, \quad (25)$$

where  $\tau_t$  in (25) is the total propagation delay. We also define the loop-transfer matrix:

$$L = P_{12} X Q_{21}. \quad (26)$$

The equivalent representation of Fig. 9(a) is given in Fig. 9(b), where the MIMO loop-transfer matrix  $L$  is connected by feedback via the time-delay block  $\mathcal{D}_t$ . General stability results do not exist for such a problem in the multivariable case.

A possible approach is to use an LTI approximation for the time-delay part, such as Padé approximation. This approach is taken in the following. The basic idea is to isolate the unknown time-delay as a real block diagonal uncertainty, to rearrange the system in a  $M\Delta$  structure, where  $M$  is the transfer matrix from the output to the input of the perturbation, and then to use robust stability and  $\mu$ -analysis results.

**Theorem 4.** *Under (A1), optical network stability in Fig. 3 (or Fig. 5) is equivalent to robust stability of the closed-loop system in Fig. 10(b). Therefore, the closed-loop system is stable if and only if*

$$\sup_{\omega} \mu_{\Delta}(M(j\omega)) < \beta \quad \forall \omega \quad (27)$$

for all  $\Delta$  such that  $\|\Delta\|_{\infty} \leq \frac{1}{\beta}$ , where

$$M(s) = F_l(G_{x,\text{Pade}}(s), L(s))$$

is assumed stable, with  $L(s)$  being the loop transfer matrix, (26), and  $G_{x,\text{Pade}}(s)$  the nominal Padé approximation of  $\mathcal{D}_t$ , (25).

**Proof.** Recall that the equivalent representation for network stability analysis is shown in Fig. 9(b), with  $L, \mathcal{D}_t$  as in (26),(25). Let the delay  $\tau_t$  be expressed as

$$\tau_t = \tau_0 + \delta_0 \delta, \quad \delta \in [-1, 1] \quad (28)$$

with  $\tau_0$  nominal delay,  $\delta_0$  a known scalar, and  $\delta$  an unknown, bounded real scalar. Let a single-channel delay  $e^{-\tau_t s}$  be approximated by a Padé LTI system,  $H_{\text{Pade}}(s)$ , which is expressed as an upper LFT of a generalized plant  $G_{g,\text{Pade}}$  by a real uncertainty  $\delta$

$$H_{\text{Pade}}(s) = F_u(G_{g,\text{Pade}}(s), \delta).$$

Under (A1), the multichannel delay,  $\mathcal{D}_t(s)$ , Fig. 9(b), is expressed therefore as

$$H_{x,\text{Pade}}(s) = F_u(G_{x,\text{Pade}}(s), \Delta), \quad \Delta = \delta * I_{m_1}$$

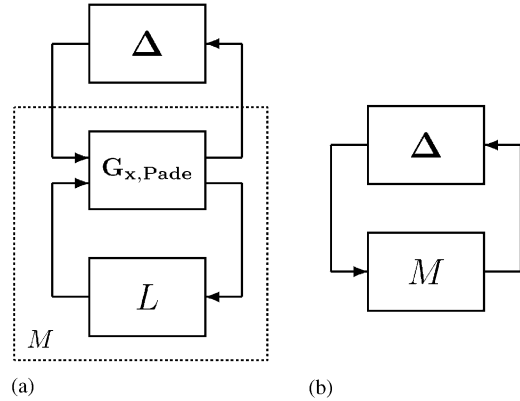


Fig. 10.  $M\Delta$  configuration for network stability.

with  $\delta \in [-1, 1]$ , and  $G_{x,\text{Pade}}(s)$ , block-diagonal as

$$G_{x,\text{Pade}}(s) = \begin{bmatrix} G_{g,\text{Pade}}(s) & \cdots & 0 \\ & \ddots & \\ 0 & \cdots & G_{g,\text{Pade}}(s) \end{bmatrix}.$$

Then the configuration in Fig. 9(b) is equivalent to Fig. 10(a), and the result follows from standard small gain theorem and  $\mu$ -analysis theory, (see Packard & Doyle, 1993; Zhou et al., 1996). Since the block diagrams in Fig. 10(a) and (b) are equivalent, stability of the closed-loop system in Fig. 10(a) is equivalent to robust stability of the system in Fig. 10(b), assuming that

$$M = F_l(G_{x,\text{Pade}}, L)$$

is stable. Then use of robust stability condition (27) ensures network stability.  $\square$

**Remark 7.** Note that a state-space realization for the generalized plant  $G_{g,\text{Pade}}$  can be found depending on the approximation order, i.e., on the order of  $H_{\text{Pade}}(s)$ . For example, for a first-order Padé approximation

$$H_{\text{Pade}}(s) = \frac{-\tau_t s/2 + 1}{\tau_t s/2 + 1}$$

we have

$$G_{g,\text{Pade}}(s) = \begin{bmatrix} A_g | B_g \\ \hline C_g | D_g \end{bmatrix} \quad \text{with}$$

$$A_g = -\frac{2}{\tau_0}, \quad B_g = \begin{bmatrix} -\frac{\delta_0}{\tau_0} & \frac{4}{\tau_0} \end{bmatrix},$$

$$C_g = \begin{bmatrix} -\frac{2}{\tau_0} \\ 1 \end{bmatrix}, \quad D_g = \begin{bmatrix} -\frac{\delta_0}{\tau_0} & \frac{4}{\tau_0} \\ 0 & -1 \end{bmatrix}.$$

**Remark 8.** This robust stability problem is in the class of repeated real diagonal perturbations, i.e., uncertainty in each channel is identical. The  $\mu$  value gives the magnitude of the tolerated perturbation before instability,

$$\|A\|_{\infty} \leq \frac{1}{\beta_l},$$

where  $\beta_l$  is the peak of the  $\mu$  lower bound, (see Packard & Doyle, 1993). This gives the maximum delay  $\bar{\tau}$ , (28), or maximum path length, before instability,

$$\bar{\tau} = \tau_0 + \delta_0 \frac{1}{\beta_l}.$$

Theorem 4 is the first theoretical result for optical network stability, based on a linearized model. An interesting extension would be to use a nonlinear model and Lyapunov techniques for time-delay systems (see Niculescu, 2001).

## 5. Simulation results

Consider a network configuration as in Fig. 1, with twelve optical dynamic amplifier spans, each span of approximately 70 km, corresponding to about  $\tau = 0.33$  ms delay. The network has 80 wavelengths grouped in 10 sub-bands propagating across a total  $12 \times 70$  km loop, resulting in a total nominal delay of about  $\tau_0 = 4$  ms. Each dynamic optical amplifier is composed of an optical amplifier (EDFA) and a DGE, which is modeled as a wavelength decoupled system. Each EDFA is modeled as a  $(10 \times 10)$  MIMO transfer matrix with high-pass diagonal terms, and low-pass off-diagonal terms.

We assume that the two groups  $\lambda_1$  and  $\lambda_2$  are equal, and are added at  $t = -\infty$  so that at  $t = 0$  the system has reached equilibrium. At  $t = 50 \mu\text{s}$  a sudden increase in power occurs on the  $\lambda_2$  group with a 1.5 dB tilt. Results are shown in Fig. 11(a) and (b) for the case when the loop time-delay (loop path length) is varied. For the case when time-delay is four times larger  $\tau_t = 16$  ms, Fig. 11(b), the network becomes unstable, with sustained bursts of power fluctuations or oscillations. This corresponds to previous results on physical networks, (see Kim et al., 2000; Pavel, 2002). Using Theorem 4, we can obtain an estimate of the maximum delay before instability. Numerical calculation using the  $\mu$  toolbox in Matlab gives  $\mu = 1.05$  yielding a destabilizing perturbation of  $\bar{\tau}_t \approx 15$  ms. This shows that Theorem 4 provides a good estimate although slightly conservative.

## 6. Conclusions

In this paper, we have developed an analytical approach for studying dynamic behavior in optical networks. To our knowledge, this represents the first theoretical study of dynamic response in optical networks, from a control theory perspective. Such a problem is extremely complex as the optical network is a large-scale multivariable, interconnected system, with distributed time-delays. This work is relevant

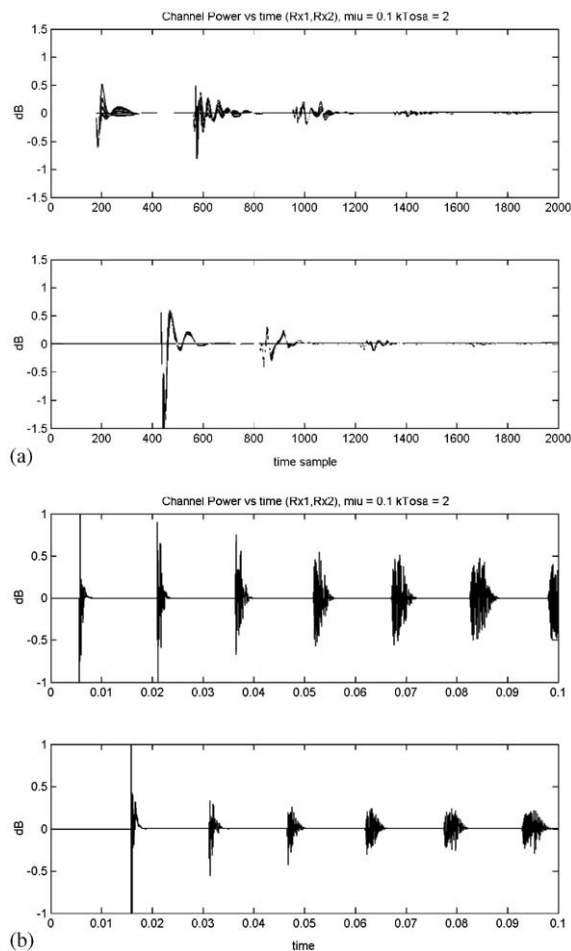


Fig. 11. Simulation results for: (a) nominal, (b) four times larger time-delay.

for reconfigurable optical networks where closed cycles, affected by time-delay, can be formed.

We found a closed-form expression of the network transfer matrix, by resorting to linear fractional transformation techniques. Under the natural assumption of equal time-delay for all channels in a link this expression was simplified such that cross-coupling is evidenced. We derived some network stability conditions, obtained by reformulating the problem as a robust stability problem and resorting to  $\mu$ -analysis.

## References

- Agrawal, G. P. (2002). *Fiber-optic communication systems*. New York: Wiley.
- Alpcan, T., & Basar, T. (2002). A game-theoretic framework for congestion control in general topology networks. *Proceedings of the 41st IEEE conference on decision and control*, Las Vegas, NV (pp. 1218–1223).
- Altman, E., Basar, T., & Srikant, R. (1999). Congestion control as a stochastic control problem with action delays. *Automatica*, 35, 1937–1950.

- Anderson, B. D. O. (1973). *Network analysis and synthesis—a modern systems theory approach*. Englewood Cliffs, NJ: Prentice-Hall.
- Bala, K., & Brackett, C. A. (1996). Cycles in wavelength routed optical networks. *IEEE Journal of Lightwave Technology*, 14, 1585–1594.
- Barnes, S. (2002). All-optical networks: Principles, solutions and challenges. *Proceedings of optical fiber communication conference*, Anaheim, CA (pp. 98–99).
- Ford, J. E., & Walker, J. A. (1998). Dynamic spectral power equalization using micro-optomechanics. *IEEE Photonics Technology Letters*, 10, 1440–1442.
- Kim, P., Bae, S., Joon Ahn, S., & Park, N. (2000). Analysis on the channel power oscillation in the closed WDM ring network with the channel power equalizer. *IEEE Photonics Technology Letters*, 12, 1409–1411.
- Mukherjee, B. (2000). WDM optical communication networks: Progress and challenges. *IEEE Journal on Selected Areas in Communications*, 18, 1810–1824.
- Niculescu, S.-I. (2001). *Delay effects on stability—a robust control approach*. Berlin, Germany: Springer.
- Packard, A., & Doyle, J. C. (1993). The complex structured singular value. *Automatica*, 29, 71–109.
- Pavel, L. (2002). Effect of equalization strategy on dynamic response of optical networks. *Proceedings of IEEE LEOS 2002. Laser and Electro-Optics Society annual meeting*, Glasgow, UK (pp. 185–186).
- Pavel, L. (2003). Control design for transient power and spectral control in optical communication networks. In *Proceedings of IEEE Conference for Control Applications*, Istanbul, Turkey (pp. 415–422).
- Srivastava, A. K., Sun, Y., Zyskind, J. L., & Sulhoff, J. W. (1997). EDFA transient response to channel loss in WDM transmission systems. *IEEE Photonics Technology Letters*, 9, 386–388.
- Sun, Y., Zyskind, J. L., & Srivastava, A. K. (1997). Average inversion level, modeling, and physics of Erbium-doped fiber amplifiers. *IEEE Journal on Selected Topics in Quantum Electronics*, 3, 991–1007.
- Wang, Z., & Paganini, F. (2002). Global stability with time-delay in network congestion control. *Proceedings of the 41st IEEE conference on decision and control*, Las Vegas, NV (pp. 3632–3637).
- Yoo, S. J. B., Xin, W., & Garrett, L. D. (1998). Observation of prolonged power transients in a reconfigurable multiwavelength network and their suppression by gain-clamping of optical amplifiers. *IEEE Photonics Technology Letters*, 10, 1659–1661.
- Zhou, K., Doyle, J. C., & Glover, K. (1996). *Robust and optimal control*. Upper Saddle River, NJ: Prentice-Hall.



**Lacra Pavel** has received the M. Eng. degree in Automatic Control from the Technical University Iasi, Romania in 1989 and the Ph.D. degree in Electrical Engineering (Control Theory) from Queen's University, Kingston, Canada in 1996. Between 1997 and 1998 she was with the National Research Council in Ottawa, as an NSERC Postdoctoral Fellow, working on noise and vibration control for flexible structures. From 1998 to 2002 she worked in the optical communication industry as a Senior

Control Engineer. In 2002 she joined University of Toronto, where she is currently an Assistant Professor cross-appointed to Systems Control and Optical Communications. Her research interests are in the general area of control theory with applications to optical communications networks, control of networks, robust and H-infinity optimal control, nonlinear control systems.